SUPPORTING NOTE 1

Experimental coil noise calibration

The Johnson noise that would arise from conductors in our simulated coils depends upon the detailed distribution of current through those conductors. The current patterns given by Equation [4] for loop coils or [A.23] for dipole coils assume a unit current integrated over the conductor path, and a cross-sectional current distribution a) which is uniform across the small conductor thickness d_c, and b) which would be uniform across the conductor width if the mode expansion were taken to infinite order. In practice, for finite mode order, the current follows a *sinc* shape, with an effective width (κ) that depends upon the Fourier expansion order, i.e., the largest values used for the coefficients *n* and *m*:

$$\begin{aligned} \kappa_z &= \frac{1.22\pi}{m_{max}} \qquad && \hat{\boldsymbol{z}} - directed\ conductors \\ \kappa_\varphi &= \frac{1.22\pi r_b}{n_{max}} \qquad && \hat{\boldsymbol{\varphi}} - directed\ conductors \end{aligned} \qquad [B.1]$$

These assumptions become less realistic for wider conductors and at UHF, in which case current is known to be concentrated at the edges rather than at the center of the conductors (S1). In addition, for cylindrical window loop coils, our expressions assume a uniform current along the length of the conductors, whereas actual coil current distribution may depend on many factors such as distributed capacitor arrangement, perimeter, frequency of operation, and loading conditions. As a result, Eq. [A.24] underestimates coil noise, which requires calibration to accurately compare simulations and experiments. For the results in **Figure 2**, we estimated the correction factor based on

the following procedure:

1. Calculate the inductance of a rectangular loop with the same dimensions as a coil element in the actual array (S2):

$$L^{loop} = N^2 \frac{\mu_0}{\pi}\left[-2(w+h) + 2\sqrt{h^2+w^2} - h\ln\left(\frac{h+\sqrt{h^2+w^2}}{w}\right) - w\ln\left(\frac{w+\sqrt{h^2+w^2}}{h}\right) + h\ln\left(\frac{2h}{a}\right) + w\ln\left(\frac{2w}{a}\right)\right] \quad [B.2]$$

   N is the number of turns (N = 1 in our case), a is the diameter of the conductor wire, and $w = 2l_l$ and $h = 2\varphi_0 r_b$ are the lengths of axial and azimuthal sides, respectively (**Figure 1**). Using the average conductor width of the DGF simulation set-up (Eq. [B.1]) as an estimate for the wire diameter (a = 8.7 mm), we obtained $L^{loop} = 3\times10^{-7}$ H.

2. Measure the unloaded Q of a loop coil identical to the coil elements of the actual array and calculate its resistance as (S3)

$$R^{loop} = \frac{\omega L^{loop}}{Q} \quad [B.3]$$

   We measured $Q = 260$, which resulted in $R^{loop} = 0.9\ \Omega$.

3. Calculate the radiation resistance of the array element as (S4):

$$R_r = \frac{320\pi^4}{\lambda^4}(hw)^2 \quad [B.4]$$

   where λ is the wavelength in free space. In our case, $R_r = 0.35\ \Omega$.

4. The coil noise correction factor τ_c is then calculated by applying the weights in

Eq. [4] to the simulated R_A for one loop (first diagonal element in Eq. [A.24]) and comparing the result with Eq. [B.3], after subtracting radiation losses (Eq. [B.4]) because they are not automatically included in the current DGF implementation:

$$\tau_c = \frac{R^{loop} - R_r}{R_A} \qquad [B.5]$$

We calculated $\tau_c = 1.95$ and used it to scale R_A in the simulations for **Figure 2**.

Note that the exact dimensions of the conductor wires in the actual array could not be modeled in simulation using Eq. [B.1], due to limits in the maximum expansion order allowed by Matlab's numerical precision. The effect of this discrepancy in conductor cross section was also captured by the coil noise correction factor.

SUPPLEMENTARY REFERENCES

S1. Rautio JC. An Investigation of Microstrip Conductor Loss. IEEE Microwave Magazine 2001;1:1–8.

S2. EMC Laboratory, Missouri University S&T. Rectangular Loop Inductance Calculator. http://emclab.mst.edu/inductance/rectgl/

S3. Kumar A, Edelstein WA, Bottomley PA. Noise figure limits for circular loop MR coils. Magn. Reson. Med. 2009;61:1201–1209. doi: 10.1002/mrm.21948.

S4. Evjen PM, Jonsrud GE. SRD Antennas. Texas Instruments; AN003-SWRA088. http://www.ti.com/lit/an/swra088/swra088.pdf.

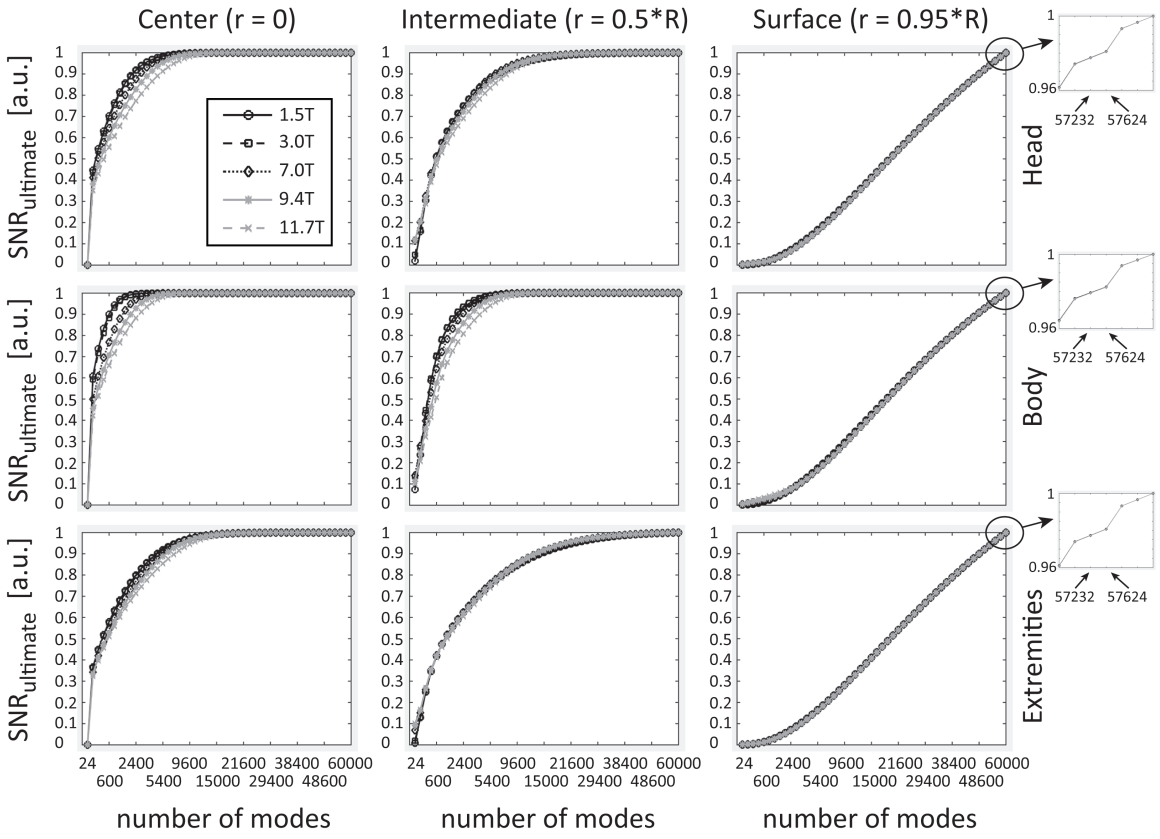

Supporting Figure S1. Convergence of the Ultimate Intrinsic SNR (UISNR) calculations. UISNR was calculated using azimuthal and axial mode expansion orders of n = – 48:1:47 and m = –150:1:149, which correspond to a basis with 57,600 surface current modes, equally divided between curl-free and divergence-free types. This ensured convergence of the calculations. The zoomed views on the right show that calculations converged also for the case of a voxel near the surface of the cylinder, although the discretization of the plots seems to suggest the contrary. In fact, UISNR changes only by 0.3% when the number of modes is increased from 57,232 to 57,624.

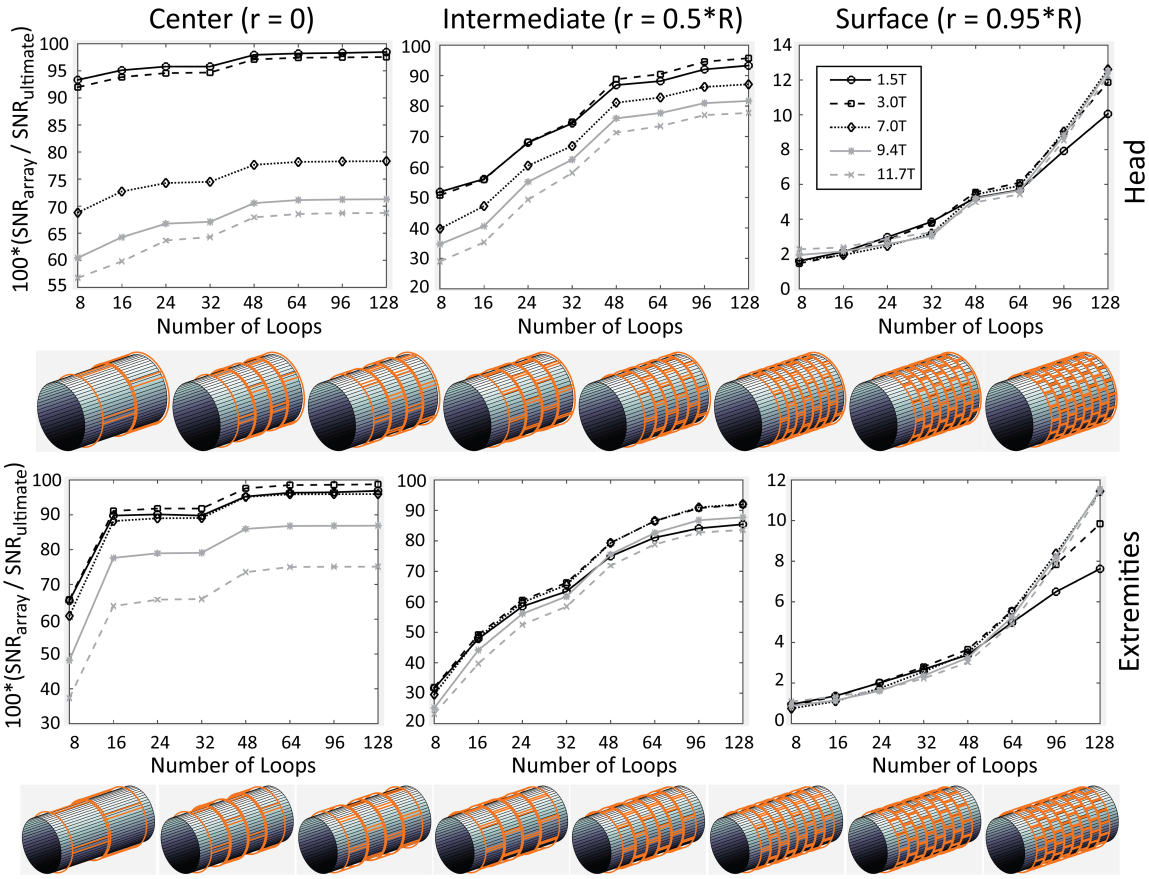

Supporting Figure S2. Coil performance as a percentage of the UISNR vs. number of loops in the array, for different values of main magnetic field strength and voxel position. Results are shown for samples with average size and electrical properties of the head (top) and extremities (bottom). Results for samples with average size and electrical properties of the human body are shown in **Figure 3.**

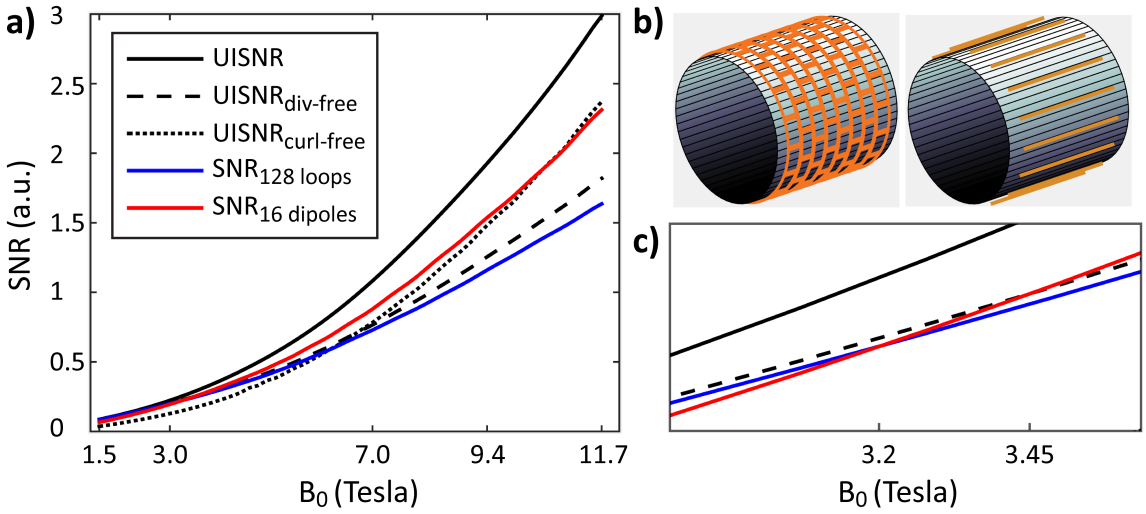

Supporting Figure S3. UISNR and SNR of finite arrays at the center *vs.* main magnetic field strength (a). Array geometries for a body-size sample are shown in (b). The SNR of the array with 16 dipoles exceeded that of the array with 128 loops for B_0 > 3.2 T and the UISNR achievable using either only curl-free or only divergence-free current modes for 3.45 T < B_0 < ~10.5 T (c). The array with 128 loops approached the UISNR closely only at low field.